

Experimental and Theoretical Analysis of the Pyrolysis Mechanism of a Dimeric Lignin Model Compound with α -O-4 Linkage

Chao Liu, Yubin Deng, Shubin Wu,* Ming Lei, and Jiajin Liang

In this study, 4-benzyloxyphenol was introduced as an α -O-4 dimeric lignin model compound to explore the pyrolysis mechanism of α -O-4 linkage in lignin. Pyrolysis-gas chromatography/mass spectrometry (Py-GC/MS), density functional theory (DFT) calculations, and collision theory were employed to illustrate the pyrolysis process experimentally and theoretically. The results suggest that the pyrolysis of 4-benzyloxyphenol starts from the C α -O bond homolysis because it has the lowest bond dissociation energy (BDE) (164.9 kJ/mol). Among the four main products, as well as the primary products, the formation of bibenzyl and toluene depend on the probability of molecular collisions, while the formation of *p*-benzoquinone and hydroquinone is influenced by thermodynamic factors. The minor products, which were basically generated from the secondary pyrolysis of the main products and consisted of oxygenated compounds and polycyclic compounds, were only observed at 600 °C. The energy barrier, the enthalpy change, and their combined effects determined the formation of minor products.

Keywords: Dimeric lignin model compound; α -O-4 linkage; Pyrolysis mechanism; DFT method; Collision theory

Contact information: State Key Laboratory of Pulp and Paper Engineering, South China University of Technology, Guangzhou, Guangdong 510640, PR China; *Corresponding author: shubinwu@scut.edu.cn

INTRODUCTION

With increasing depletion of fossil resources (coal, oil, and gas) and the deterioration of the environment (acid rain, greenhouse effect, ozone hole, *etc.*), new sources of energy are being sought. As a renewable and sustainable resource, biomass is considered to be a substitute for fossil resources. For this purpose, more attention has been paid to the development and utilization of biomass in recent decades. Among the forms of utilization, pyrolysis is regarded as a promising method of converting biomass into bio-oil (Bridgwater *et al.* 1999). The pyrolysis of different raw materials (Jiang *et al.* 2010; Lv *et al.* 2013; Liang *et al.* 2015) with various equipment (Lédé *et al.* 2007; Guo *et al.* 2012; Zhang *et al.* 2013) with factors such as temperature (Jiang *et al.* 2010; Lou *et al.* 2010), residence time (Marsh *et al.* 2004; Guo and Wang 2015), additive and catalyst (Guo *et al.* 2012; Zhang *et al.* 2013; Shao *et al.* 2014), and atmosphere (Chen *et al.* 2008), has been widely investigated. However, the intermediate pyrolysis processes are still obscure. Hence, it is necessary to investigate the pyrolysis mechanism of biomass.

Because of its diverse composition, biomass has complicated pyrolysis reactions. Therefore, a mechanistic study on a single component of biomass is realistic. Of the three major components of biomass (cellulose, lignin, and hemicellulose), lignin has a more

complex chemical structure and pyrolysis mechanism than cellulose (Shen and Gu 2009) or hemicellulose (Wang *et al.* 2013), whose pyrolysis mechanisms have been thoroughly investigated already. Therefore, for the in-depth understanding of biomass pyrolysis, it is necessary to explore the mechanism of lignin pyrolysis. Furthermore, in the process of exploring the pyrolysis mechanism, pyrolysis-gas chromatography/mass spectrometry (Py-GC/MS) is widely used because of its speediness and repeatability (Guo and Wang 2015). In addition, for the further understanding of the lignin pyrolysis mechanism in theory, density functional theory (DFT) is often introduced to determine the pyrolysis active site and the potential energy (Beste and Buchanan 2009; Kim *et al.* 2011; Huang *et al.* 2014a).

Lignin is composed of methoxylated phenylpropane units, including *p*-coumaryl alcohols, coniferyl alcohols, and sinapyl alcohols, which are crosslinked by ether bonds (β -O-4, α -O-4, 4-O-5') and carbon-carbon bonds (β -5, 5-5', β -1, β - β') (Kang *et al.* 2013). Among these bonds, the content of the β -O-4 linkage is the highest (45% to 60%) (Adler 1977; Chakar and Ragauskas 2004; Rodrigues Pinto *et al.* 2010; Shen *et al.* 2010; Pandey and Kim 2011). Therefore, in previous mechanism studies, dimeric lignin model compounds with β -O-4 linkage were preferred as research objects (Drage *et al.* 2002; Liu *et al.* 2011; Chu *et al.* 2013). The α -O-4 linkage, namely the second most abundant ether bond, also has a relatively high chemical activity, similar to the β -O-4 linkage, and can affect the pyrolysis process and products distribution as well. However, studies on this topic are rare, and the corresponding results only based on the experiments (Kawamoto *et al.* 2007; Kim *et al.* 2014). Hence, exploring the pyrolysis of the α -O-4 linkage experimentally and theoretically is meaningful for the further investigation of the pyrolysis mechanism of lignin.

Therefore, in this study, Py-GC/MS was introduced to identify the pyrolytic products from the α -O-4 dimeric lignin model compound. Moreover, DFT calculations and collision theory were applied to speculate on the pyrolysis process of feedstock and simulate the pyrolysis mechanism of the α -O-4 linkage in lignin.

EXPERIMENTAL

Material

The model compound used in this study was 4-benzyloxyphenol, which can be regarded as an analogue for dimeric structures within lignin. It was purchased from Aladdin Industrial Corporation (Shanghai, China) and used directly without further purification. Figure 1 shows the chemical structural formula of the α -O-4 lignin dimer model.

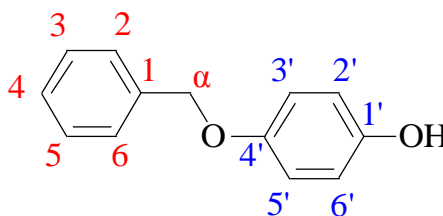


Fig. 1. Chemical structural formula of 4-benzyloxyphenol

Py-GC/MS method

Py-GC/MS was evaluated on a CDS 5200 pyrolyzer (CDS Analytical, USA) connected to a 7890A gas chromatograph coupled with a 5975C mass spectrometer (Agilent Technologies, USA). The sample was pyrolyzed at the set temperatures of (400, 500, and 600 °C) for 15 s with a heating rate of 10000 °C/s using helium as the carrier gas. The split ratio was 50:1, and the flow rate was 1.00 mL/min. The Py oven was set at 100 °C as to not volatilize the feedstock, and all others (the injector, detector, and interface temperatures) were set at 250 °C. HP-5MS capillary column (30 m × 0.25 mm × 0.25 μm, Agilent Technologies, USA) was selected as the separation column. The column temperature was programmed from 50 to 250 °C (5 min) with a heating rate of 8 °C/min. The mass spectrometer was set at an ionizing voltage of 70 eV, and the mass range from m/z 5 to 400 was scanned with a speed of 1.0 s/decade.

DFT Calculations

DFT calculations were carried out on the Gaussian 03 program (Frisch *et al.* 2004). A B3LYP/6-31G(d,p) basis set was used to optimize the equilibrium geometries of reactants, intermediates, transition states, and products (Huang *et al.* 2014b). The transition states were located by transition state theory method and were confirmed by visual inspection of the imaginary frequency using Gauss view and IRC calculations. Activation energies (reaction energy barriers) for reactions were estimated with the relative energies, including the zero-point energy correction, between the transition state and the reactant. For homolytic reactions that had no transition states, bond dissociation energy was used as a substitute for the activation energy.

RESULTS AND DISCUSSION

Pyrolytic Products Distribution

The GC/MS chromatograms of 4-benzyloxyphenol pyrolysis at 400, 500, and 600 °C are shown in Fig. 2. In these chromatograms, the volatilization of the feedstock can be clearly recognized during pyrolysis, and changes in the species and yields of pyrolytic products from 4-benzyloxyphenol are also intuitively displayed with increasing temperature. Yields (percentage of integral area) of the detected compounds after volatilized feedstock deduction are summarized in Table 1.

From Fig. 2 and Table 1, it can be seen that at 400 °C, only bibenzyl was detected. Hence, the relative yield of bibenzyl was 100%. When the temperature rose to 500 °C, the yield of bibenzyl decreased quickly to 51.42%. At the same time, toluene, *p*-benzoquinone, and hydroquinone were generated in large quantities. However, the species of pyrolytic products at 600 °C was up to 11 and the major products were still bibenzyl, toluene, *p*-benzoquinone, and hydroquinone, whose total yields were up to 98.51%. As for these minor products formed at 600 °C, the related yields were quite low; and with the exception of (*E*)-stilbene (0.78%), the yields of other minor products were approximately 0.1%.

Judging from the chemical structure of these pyrolytic products, a relationship can be proposed in which the four main compounds (bibenzyl, toluene, *p*-benzoquinone, and hydroquinone) are separately derived from the benzyl unit and the hydroquinone unit in 4-benzyloxyphenol. This assumes that these main products were produced from the

cleavage of the α -O-4 linkage in 4-benzyloxyphenol. Also, the minor products may have benefitted from the secondary pyrolysis of these main compounds.

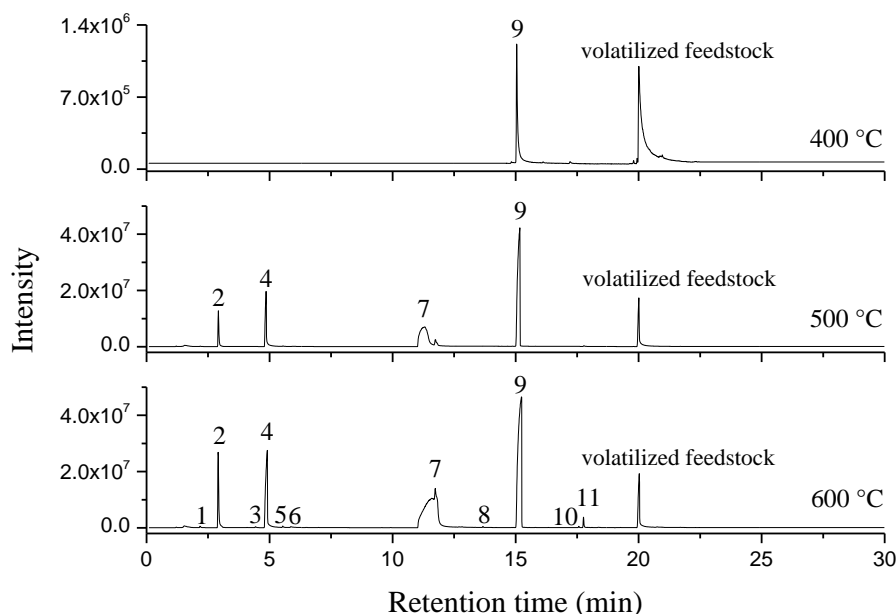


Fig. 2. GC/MS chromatograms of 4-benzyloxyphenol pyrolysis at 400, 500, and 600 °C

Table 1. Pyrolytic Products from 4-Benzyloxyphenol Detected by Py-GC/MS at Various Temperatures

Peak	RT/min	Compound ^a	Qual.	Relative content (area %)		
				400 °C	500 °C	600 °C
1	2.18	Benzene	91	-	-	0.13
2	2.92	Toluene	95	-	5.86	6.53
3	4.43	Styrene	97	-	-	0.09
4	4.90	<i>p</i> -Benzoquinone	95	-	13.14	13.31
5	5.54	Benzaldehyde	95	-	-	0.16
6	5.87	Phenol	91	-	-	0.17
7	11.60	Hydroquinone	91	-	29.58	38.11
8	13.68	Diphenylmethane	96	-	-	0.07
9	15.22	Bibenzyl	90	100.00	51.42	40.56
10	17.58	9,10-Dihydrophenanthrene	96	-	-	0.09
11	17.76	(E)-Stilbene	98	-	-	0.78

^a volatilized feedstock was deleted.

-: Not detected.

Primary Products Formation

Previous theoretical research has shown that the bond dissociation energies (BDEs) of ether linkages in lignin and its model compounds are lower than those of other linkages. Thus, these ether bonds are considered to be the active sites of lignin pyrolysis (Beste and Buchanan 2009; Kim *et al.* 2011; Huang *et al.* 2014a). For our research object, the calculated BDEs of main bonds (except for the Ar-H bonds) are listed in Table 2. As

can be seen from the data, the C_{α} -O bond has the lowest BDE (164.9 kJ/mol) and was considered to be the active site for the primary reaction. Therefore, the thermal degradation of 4-benzyloxyphenol was considered to start from the C_{α} -O bond dissociation.

Table 2. Dissociation Energy of the Main Bonds in 4-Benzyloxyphenol (kJ/mol)

Bond Type	BDE
C_1 - C_{α}	380.6
C_{α} -O	164.9
O- $C_{4'}$	449.3
C_1 -O	379.3
O-H	298.4

The pyrolysis process of 4-benzyloxyphenol is indicated in Fig. 3, which combines the experimental results and free-radical theory. As shown in Fig. 3, homolytic cleavage of the C_{α} -O bond was found in the fast pyrolysis condition. The benzyl radical (intermediate A, abbreviated IMA) and the hydroquinone radical (IMB) were generated from homolysis. Because of the homolytic reaction, the energy barrier of this step (S1) was the BDE of the C_{α} -O bond, 164.9 kJ/mol.

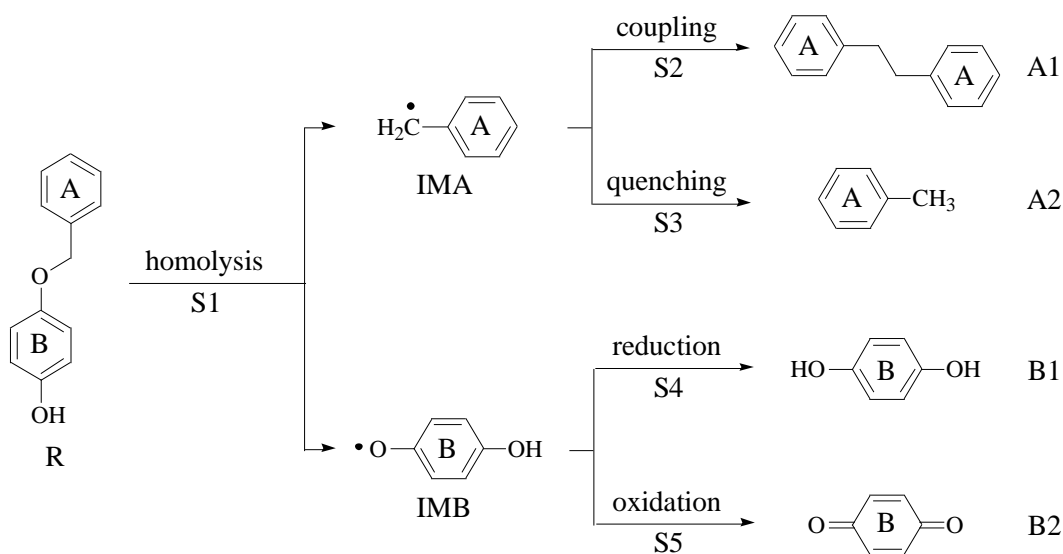


Fig. 3. Formation processes of main pyrolytic products from 4-benzyloxyphenol

Molecular collision is the basis for the further reactions of the generated IMA. When two IMA approached each other, the coupling reaction was realized with the formation of the C_{α} - $C_{\alpha'}$ bond and bibenzyl (A1). During the coupling step, the released energy was 238.9 kJ/mol. Thus, the total enthalpy change of A1 formation was less than 0 (-74.0 kJ/mol). As shown in Table 1, A1 was a major product. Therefore, the possibility of this thermodynamic process was highly in accordance with the experimental results. Furthermore, the IMA collided with the H radical and was quenched into toluene (A2). The total enthalpy change of A2 formation was -197.0 kJ/mol. The quenching pathway was also an exothermic process.

As for these two products, A1 and A2 both originated from the aryl ring A (Fig. 3). The energy barriers of the two pathways were the same. The released energy in the quenching step was more than that in the coupling step, but the experimental yield of A1 was much higher than that of A2. The inconsistency was caused by the probability of collision. After the C α -O bond break, large amounts of IMA were formed while there were not enough H radicals in the system. Hence, the probability of coupling was much higher than that of quenching and the actual yield of A1 was higher than that of A2. Overall, the experimental results provided a strong support for the collision theory.

When the collision theory was introduced to explain the further reactions of IMB, it was found that the active peroxide bond (-O-O-) would form by the coupling reaction of two IMB. However, the generated peroxide bond was broken up into IMB under the pyrolysis condition. Hence, it is not necessary to discuss the coupling reaction in IMB. Furthermore, the bimolecular disproportionation reaction should be found in IMB with hydroquinone (B1) and *p*-benzoquinone (B2) both formed equally. This process was not in accordance with the experimental results.

To explain the formation of B1 and B2, thermodynamic factors should be introduced. The generated IMB could combine with the H radical and be reduced into B1. Meanwhile, H radical could be removed with IMB, being oxidized into B2. Because of the different energy requirements for the reduction and oxidation reactions (-304.9 and 227.2 kJ/mol, respectively), the gap between the total enthalpy change of B1 formation and B2 formation was large. The formation route of B1 was an exothermic process with an energy of 140.0 kJ/mol released, while the formation of B2 was an endothermic reaction, which needed energy of 392.1 kJ/mol. The thermodynamic explanation agreed with the experimental results in Table 1, in which the yield of B1 was several times greater than that of B2.

Secondary Products Formation

Minor products were thought to be generated from the secondary pyrolysis of the primary products. The formation of secondary products is inevitable but ideally should be avoided during the thermal conversion of biomass. For example, with 4-benzyloxyphenol, some oxygenated compounds (*e.g.* benzaldehyde and phenol), and polycyclic compounds (*e.g.*, diphenylmethane and 9,10-dihydrophenanthrene) were observed at 600 °C. However, decreasing the oxygen content and the yields of polycyclic compounds is the focus of bio-oil upgrading. Hence, the formation mechanisms of these oxygenated and polycyclic compounds deserve to be discussed.

There is no doubt that phenol (B3) was formed through the dehydroxylation reaction in B1 (Fig. 4). However, the total enthalpy change of B3 formation was low (-154.4 kJ/mol) and the energy barrier of the dehydroxylation reaction approached 447.3 kJ/mol, which severely restricted the formation of B3.

As shown in Fig. 5, the active IMA also combined with the OH radical to form benzyl alcohol (IM2). The generated IM2 went on being oxidized into benzaldehyde (A3) under the thermochemical condition through the transition state 1 (TS1). The formation of the CHO group is a common reaction type in hydroxyl compounds pyrolysis (Harman-Ware *et al.* 2013; Kotake *et al.* 2013). The total enthalpy change of A3 formation was 300.3 kJ/mol. This reaction process was considered the oxidation of the benzyl radical, which was a transferring form of the oxygen during pyrolysis. The formation of A3 originated from the combination of the OH radical; therefore, the yield

of A3 was determined by the possibility of the combination, which was related to the concentration of the OH radical. Thereby, the formation of A3 was controlled by the OH radical. When the pyrolysis temperature was set at 600 °C, phenol (B3) was produced, which released an equal amount of OH radical (Fig. 4). These OH radicals contributed to the formation of A3. Furthermore, almost the same yield of B3 and A3, as listed in Table 1, further confirmed the formation pathways shown in Figs. 4 and 5.

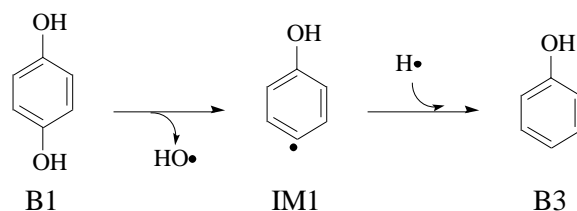


Fig. 4. Secondary pyrolysis of hydroquinone

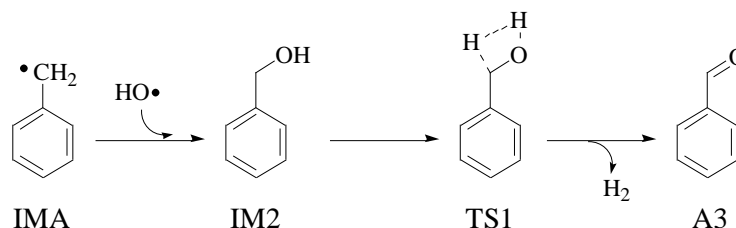


Fig. 5. Proposed formation pathway of benzaldehyde

As the most abundant pyrolytic product, bibenzyl (A1) had the highest probability to undergo secondary reactions. Other minor products were realized from the further degradation of A1. As shown in Fig. 6, secondary reactions on A1 were divided into three processes, including the homolysis of the C₁-C_α bond (Fig. 6(a)), the formation of the C₂-C_{2'} bond (Fig. 6(b)), and the formation of the C_α=C_{α'} bond (Fig. 6(c)). Inevitably, the C_α-C_α bond was broken down during pyrolysis and IMA was formed. Then, the generated IMA reacted along the routes mentioned above, therefore, these details were not repeated.

The energy barrier of the homolytic pyrolysis of the C₁-C_α bond in A1 was 402.5 kJ/mol. After the homolysis, a phenethyl radical (IM3) and a phenyl radical (IM4) were formed. Because of the lack of H radical in the system, the subsequent reaction of IM3 had to undergo the route with high-energy barrier to produce styrene (A4) (Fig. 6(a)). Hence, the total enthalpy change of A4 formation reached 458.8 kJ/mol.

Because of the active chemical structure, the generated IM4 would combine with other radicals. As determined from the experimental products in Table 1, IM6 might be quenched into benzene (A5) by the H radical, which would release energy of 456.7 kJ/mol. The active IM6 might react with OH radical as well, with phenol (A6/B3) formed and energy of 449.6 kJ/mol released. In addition, IM6 could even combine with the benzyl radical (IMA), transferred into diphenylmethane (A7), which would release energy of 344.2 kJ/mol.

Although the yield of 9,10-dihydrophenanthrene (A8) was low, only 0.09%, it might be transferred into phenanthrene through dehydrogenation. Phenanthrene could be further polymerized into polycyclic compounds and induce the coke formation. Hence, it was necessary to investigate the formation of A8. Figure 6(b) gave out the formation

pathway of A8. Firstly, the C_{α} - $C_{\alpha'}$ bond was twisted to let C_2 and C_2' get close. Then, the C_2 - C_2' bond was formed through a cyclic transition state. The energy barrier of A8 formation was 500.5 kJ/mol, which severely restricted the formation of A8.

As the most abundant secondary product, (E)-stilbene (A9) was produced along Fig. 6(c). The formation pathway of A9 was also an endothermic process, whose total enthalpy change was 441.2 kJ/mol and energy barrier only 351.4 kJ/mol, which was lower than any other barriers during the secondary pyrolysis.

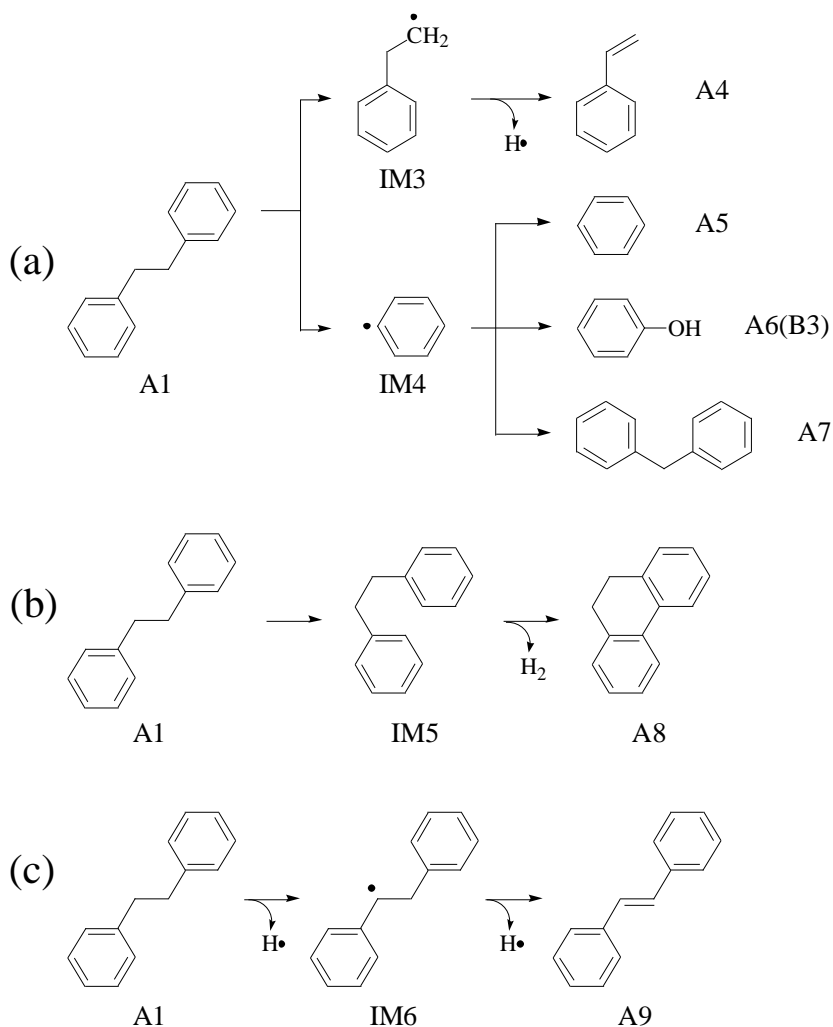


Fig. 6. Secondary pyrolysis of bibenzyl: (a) homolysis of the C_1 - C_{α} bond, (b) formation of the C_2 - C_2' bond, and (c) formation of the C_{α} = $C_{\alpha'}$ bond.

CONCLUSIONS

A dimeric lignin model compound with α -O-4 linkage was investigated by experiments (Py-GC/MS) and theories (DFT calculations and collision theory) in order to explore the pyrolysis mechanism of lignin. The following results could make the α -O-4 linkage dissociation and the subsequent pyrolysis reactions much clearer.

1. The DFT results suggested that the BDE of the C_α-O bond in 4-benzyloxyphenol was the lowest (164.9 kJ/mol). Thus, pyrolysis started from the C_α-O bond homolysis, which was consistent with the Py-GC/MS results.
2. Among pyrolytic products, bibenzyl, toluene, *p*-benzoquinone, and hydroquinone were the main products. The formation of bibenzyl and toluene depended on the probability of molecular collision; while the formation of *p*-benzoquinone and hydroquinone were influenced by the thermodynamic factors.
3. Small amounts of oxygenated compounds and polycyclic compounds were produced from the secondary pyrolysis of main products at 600 °C. The energy barriers and total enthalpy changes of the minor products formation were high, which led to their low yields.

ACKNOWLEDGMENTS

This work was supported by the National Major Fundamental Research Program of China (973 program, No. 2013CB228101) and the State Natural Sciences Foundation of China (No. 31270635).

REFERENCES CITED

- Adler, E. (1977). "Lignin chemistry—Past, present and future," *Wood Sci. Technol.* 11(3), 169-218. DOI: 10.1007/BF00365615
- Beste, A., and Buchanan, A. C. (2009). "Computational study of bond dissociation enthalpies for lignin model compounds. Substituent effects in phenethyl phenyl ethers," *J. Org. Chem.* 74(7), 2837-2841. DOI: 10.1021/jo9001307
- Bridgwater, A. V., Meier, D., and Radlein, D. (1999). "An overview of fast pyrolysis of biomass," *Org. Geochem.* 30(12), 1479-1493. DOI: 10.1016/S0146-6380(99)00120-5
- Chakar, F. S., and Ragauskas, A. J. (2004). "Review of current and future softwood kraft lignin process chemistry," *Ind. Crops Prod.* 20(2), 131-141. DOI: 10.1016/j.indcrop.2004.04.016
- Chen, Y., Duan, J., and Luo, Y. (2008). "Investigation of agricultural residues pyrolysis behavior under inert and oxidative conditions," *J. Anal. Appl. Pyrol.* 83(2), 165-174. DOI: 10.1016/j.jaap.2008.07.008
- Chu, S., Subrahmanyam, A. V., and Huber, G. W. (2013). "The pyrolysis chemistry of a β-O-4 type oligomeric lignin model compound," *Green Chem.* 15(1), 125-136. DOI: 10.1039/C2GC36332A
- Drage, T. C., Vane, C. H., and Abbott, G. D. (2002). "The closed system pyrolysis of β-O-4 lignin substructure model compounds," *Org. Geochem.* 33(12), 1523-1531. DOI: 10.1016/S0146-6380(02)00119-5
- Frisch, M. J., Trucks, G. W., Schlegel, H. B., Scuseria, G. E., Robb, M. A., Cheeseman, J. R., Montgomery, J. A., Vreven, T., Jr., Kudin, K. N., Burant, J. C., *et al.* (2004). Gaussian 03, Revision E.01, Gaussian, Inc., Wallingford, CT.
- Guo, X., and Wang, S. (2015). "Mechanism research on fast pyrolysis of organosolv lignin by pyrolyzer coupled with gas chromatography and mass spectrometry," *J.*

- Renew. Sustain. Energ.* 7(2), 023116. DOI: 10.1063/1.4916633
- Guo, D., Wu, S., Liu, B., Yin, X., and Yang, Q. (2012). "Catalytic effects of NaOH and Na₂CO₃ additives on alkali lignin pyrolysis and gasification." *Appl. Energ.* 95, 22-30. DOI: 10.1016/j.apenergy.2012.01.042
- Harman-Ware, A. E., Crocker, M., Kaur, A. P., Meier, M. S., Kato, D., and Lynn, B. (2013). "Pyrolysis–GC/MS of sinapyl and coniferyl alcohol," *J. Anal. Appl. Pyrol.* 99, 161-169. DOI:10.1016/j.jaap.2012.10.001
- Huang, J., Liu, C., Jin, Q., Tong, H., Li, W., and Wu, D. (2014a). "Density functional theory study on bond dissociation enthalpies for lignin dimer model compounds," *J. Renew. Sustain. Energ.* 6(3), 033116. DOI: 10.1063/1.4880213
- Huang, J., Liu, C., Wu, D., Tong, H., and Ren, L. (2014b). "Density functional theory studies on pyrolysis mechanism of β -O-4 type lignin dimer model compound," *J. Anal. Appl. Pyrol.* 109, 98-108. DOI: 10.1016/j.jaap.2014.07.007
- Jiang, G., Nowakowski, D. J., and Bridgwater, A. V. (2010). "Effect of the temperature on the composition of lignin pyrolysis products," *Energy Fuel* 24(8), 4470-4475. DOI: 10.1021/ef100363c
- Kang, S., Li, X., Fan, J., and Chang, J. (2013). "Hydrothermal conversion of lignin: A review," *Renew. Sustain. Energ. Rev.* 27, 546-558. DOI: 10.1016/j.rser.2013.07.013
- Kawamoto, H., Horigoshi, S., and Saka, S. (2007). "Pyrolysis reactions of various lignin model dimers," *J. Wood Sci.* 53, 168-174. DOI: 10.1007/s10086-006-0834-z
- Kim, K. H., Bai, X., and Brown, R. C. (2014). "Pyrolysis mechanisms of methoxy substituted α -O-4 lignin dimeric model compounds and detection of free radicals using electron paramagnetic resonance analysis," *J. Anal. Appl. Pyrol.* 110, 254-263. DOI: 10.1016/j.jaap.2014.09.008
- Kim, S., Chmely, S. C., Nimlos, M. R., Bomble, Y. J., Foust, T. D., Paton, R. S., and Beckham, G. T. (2011). "Computational study of bond dissociation enthalpies for a large range of native and modified lignins," *J. Phys. Chem. Lett.* 2(22), 2846-2852. DOI: 10.1021/jz201182w
- Kotake, T., Kawamoto, H., and Saka, S. (2013). "Pyrolysis reactions of coniferyl alcohol as a model of the primary structure formed during lignin pyrolysis," *J. Anal. Appl. Pyrol.* 104, 573-584. DOI: 10.1016/j.jaap.2013.05.011
- Lédé, J., Broust, F., Ndiaye, F., and Ferrer, M. (2007). "Properties of bio-oils produced by biomass fast pyrolysis in a cyclone reactor," *Fuel* 86(12-13), 1800-1810. DOI: 10.1016/j.fuel.2006.12.024
- Liang, J., Lin, Y., Wu, S., Liu, C., Lei, M., and Zeng, C. (2015). "Enhancing the quality of bio-oil and selectivity of phenols compounds from pyrolysis of anaerobic digested rice straw," *Bioresour. Technol.* 181, 220-223. DOI: 10.1016/j.biortech.2015.01.056
- Liu, J., Wu, S., and Lou, R. (2011). "Chemical structure and pyrolysis response of β -O-4 lignin model polymer," *BioResources* 6(2), 1079-1093. DOI: 10.15376/biores.6.2.1079-1093
- Lou, R., Wu, S., and Lv, G. (2010). "Effect of conditions on fast pyrolysis of bamboo lignin," *J. Anal. Appl. Pyrol.* 89(2), 191-196. DOI: 10.1016/j.jaap.2010.08.007
- Lv, G., Wu, S., Yang, G., Chen, J., Liu, Y., and Kong, F. (2013). "Comparative study of pyrolysis behaviors of corn stalk and its three components," *J. Anal. Appl. Pyrol.* 104, 185-193. DOI: 10.1016/j.jaap.2013.08.005
- Marsh, N. D., Ledesma, E. B., Sandrowitz, A. K., and Wornat, M. J. (2004). "Yields of polycyclic aromatic hydrocarbons from the pyrolysis of catechol

- [ortho-dihydroxybenzene]: Temperature and residence time effects," *Energy Fuel* 18(1), 209-217. DOI: 10.1021/ef010263u
- Pandey, M. P., and Kim, C. S. (2011). "Lignin depolymerization and conversion: A review of thermochemical methods," *Chem. Eng. Technol.* 34(1), 29-41. DOI: 10.1002/ceat.201000270
- Rodrigues Pinto, P. C., Borges Da Silva, E. A., and Rodrigues, A. E. (2010). "Insights into oxidative conversion of lignin to high-added-value phenolic aldehydes," *Ind. Eng. Chem. Res.* 50(2), 741-748. DOI: 10.1021/ie102132a
- Shao, S., Zhang, H., Heng, L., Luo, M., Xiao, R., and Shen, D. (2014). "Catalytic conversion of biomass derivatives over acid dealuminated ZSM-5," *Ind. Eng. Chem. Res.* 53(41), 15871-15878. DOI: 10.1021/ie5024657
- Shen, D. K., and Gu, S. (2009). "The mechanism for thermal decomposition of cellulose and its main products," *Bioresour. Technol.* 100(24), 6496-6504. DOI: doi:10.1016/j.biortech.2009.06.095
- Shen, D. K., Gu, S., Luo, K. H., Wang, S. R., and Fang, M. X. (2010). "The pyrolytic degradation of wood-derived lignin from pulping process," *Bioresour. Technol.* 101(15), 6136-6146. DOI: 10.1016/j.biortech.2010.02.078
- Wang, S., Ru, B., Lin, H., and Luo, Z. (2013). "Degradation mechanism of monosaccharides and xylan under pyrolytic conditions with theoretic modeling on the energy profiles," *Bioresour. Technol.* 143, 378-383. DOI: 10.1016/j.biortech.2013.06.026
- Zhang, H., Xiao, R., Jin, B., Shen, D., Chen, R., and Xiao, G. (2013). "Catalytic fast pyrolysis of straw biomass in an internally interconnected fluidized bed to produce aromatics and olefins: Effect of different catalysts," *Bioresour. Technol.* 137, 82-87. DOI: 10.1016/j.biortech.2013.03.031

Article submitted: October 15, 2015; Peer review completed: January 30, 2016; Revised version received and accepted: February 19, 2016; Published: February 29, 2016.

DOI: 10.15376/biores.11.2.3626-3636